Tampere University of Applied Sciences

Synthesis of Zero-valent Iron Nanoparticles by Microfluidic Reactor for Organic Dye Treatment

Anh Nguyen

BACHELOR'S THESIS

May 2020

Degree Programme in Energy and Environmental Engineering

ABSTRACT

Tampereen ammattikorkeakoulu
Tampere University of Applied Sciences
Degree Programme in Energy and Environmental Engineering

ANH NGUYEN:
Synthesis of Zero - Valent Iron Nanoparticles by Microfluidic Reactor for Organic Dye Treatment

Bachelor's thesis 46 pages, appendices 3 pages
May 2020

The textile and garment industry has been a crucial sector to Vietnamese economy for the last five years. Since the industry relies on water resources for its production and its wastewater contains organic dyes which are hazardous to environment, it is essential that advanced technology be applied to replace old-fashioned treatment methods. Particularly, application of iron nanomaterial in textile wastewater treatment was proposed in this project.

In this study, iron nanomaterial was synthesized by a reaction of $FeCl_3$ with $NaBH_4$ using microfluidic device as a microreactor which was fabricated from polydimethylsiloxane by photolithography and soft lithography processes. The design had double spiral micromixers to ensure highest mixing rate. The morphology and structure of the as-prepared nanomaterial were characterized by scanning microscope and X-ray diffraction analyses. The collected product was zero valent iron material in the shape of nano-sheet with average thickness of approximately 50 nm. Organic dye molecules from methyl orange and methylene blue solutions could be removed by the as-prepared iron nanomaterial. The removal of dye ions was determined and assessed by the visible ultraviolet absorption spectroscopy. The absorbance was directly proportional to the amount of nanomaterial used and was impacted by pH conditions.

The removal of dye ions with iron nanomaterial synthesized by microfluidic reactor resulted in great efficiency, mostly above 80%. In addition, this new approach could minimize drawbacks of conventional methods and offer outstanding advances: even-sized nanoparticles, compact design, low operation cost, automated process, etc.

The project in the early stage still experienced difficulties and limitations, yet the overall data showed promising potential of microfluidic device in textile wastewater treatment. In the next stages, the project planned to complete final model of the device and test it with wastewater from textile factories and weaving village in Vietnam. Green chemicals were examined to replace $NaBH_4$ as well to reduce possible toxic by-products.

Key words: zero-valent iron nanomaterial, microfluidic device, organic dyes, wastewater treatment

CONTENTS

GLOSSARY or ABBREVIATIONS AND TERMS (choose one or other)

AAS	Atomic Absorption Spectroscopy
BET	Brunauer–Emmett–Teller
CFD	Computational Fluid Dynamics
CNT	Carbon Nanotube
CVOC	Chlorinated Volatile Organic Compounds
DDT	Dichlorodiphenyltrichloroethane
ICDD	International Centre for Diffraction Data
ICP-MS	Inductively Coupled Plasma Mass Spectrometry
LMB	Leuco-methylene Blue
MB	Methylene Blue
MO	Methyl Orange
MPI	Myocardial Perfusion Imaging
MRI	Magnetic Resonance Imaging
NAFOSTED	National Foundation for Science and Technology Development
nZVI	Nano Zerovalent Iron
PDMS	Polydimethylsiloxane
PVP	Polyvinylpyrrolidone
SEM	Scanning Electron Microscope
TOC	Total Organic Carbon
UV-Vis	Ultraviolet-visible
XRD	X-ray Diffraction

1 INTRODUCTION

Some of the nano concepts in nanotechnology had been mentioned during late 1800s, but not until 20th century had several advances been made in nanoscience field. The term *nanotechnology* was first defined in 1974 by Taniguchi as a branch of technology that consists of the processing of, separation, consolidation, and deformation of materials by one atom or one molecule (El Saliby et al. 2009).

The utilization of nanotechnology has been growing strongly all around the world in these last two decades due to its potential applicability in a wide range of industrial sectors such as biomedical, energy, pharmaceutical, food, agricultural, and especially environmental remediation. In terms of environmental aspect, nanotechnology can be used to enhance the treatment of contaminated soil or water and wastewater, assisting in environmental sensing or energy storage, and from then possibly promoting sustainable development as well as circular economy. In this research, the use of nanotechnology in wastewater treatment is mainly focused as this has been a red-hot issue recently. Additionally, some researching progresses indicate that the nanotechnology can be a new optimum solution towards wastewater treatment and providing sufficient drinking water worldwide with affordable costs. (Pathakoti, Manjunath & Hwang 2019, 894.)

When concerning nanomaterial nature, it can be divided into three main categories, namely *nano-adsorbents*, *nano-catalysts* and *nanomembranes*. These three types of nanomaterial are mostly utilized in removing contaminants from wastewater, which are introduced specifically below.

Nano-adsorbents are adsorbents in nanoscale which have larger surface area and larger number of active adsorption sites, compared to traditional adsorbents. These make them more ideal for wastewater treatment. Nano-adsorbents can be carbon-based, polymeric, magnetic, or nonmagnetic-based and metal oxide-based. (Pathakoti, Manjunath & Hwang 2019, 894-896.)

Nano-catalysts are widely used to enhance catalytic performance more efficiently than their bulk counterparts. For instance, TiO_2 and ZnO nanoparticles have a wide band gap of 3.2 eV which indicates their strong photocatalytic activity. They are further investigated to be utilized for degradation of organic contaminants in water. (Pathakoti, Manjunath & Hwang 2019, 894-896.)

Nanomembranes offer low energy consumption, operational cost as well as higher flux rates than reverse osmosis. They are prepared by interfacial polymerization on ultrafiltration substrates to form thin-film composite structures which are usually made of nano-zeolites, nano-Ag, nano-TiO_2 and carbon nanotubes (CNTs). (Pathakoti, Manjunath & Hwang 2019, 894-896.)

Adsorption is considered the most effective technique among oxidation, ozonation and coagulation for removal of dissolved organic pollutants in wastewater thanks to its advantages of low energy consumption, high performance capacity and eco-friendliness. Activated carbon used to be favoured as adsorbent in the past decades, yet the material is costly and hard to regenerate with low recyclability (Li et al. 2016, 2). On the other hand, zerovalent iron nanoparticles (nZVI) – one of the first-generation nanoscale environmental technology are introduced as a proper alternative adsorbent since they are nontoxic, easy to produce as well as cost-effective (Pathakoti, Manjunath & Hwang 2019, 896). Several research articles on iron nanomaterial have been published previously, yet fundamental information on iron nanoparticle properties are not well documented and synthesizing methods are still limited in peer-reviewed papers. Furthermore, there are also some drawbacks in available nZVI preparation methods that have not been overcome completely. Hence, a new approach which has been developed from former experimentations is proposed in this work as well.

1.1 Properties of Zerovalent Iron Nanoparticles

Iron nanomaterial mainly exists in superfine nanoparticles whose diameters range from 0 to 100 nm, which is approximately 10 times smaller than that of a

typical bacterial cell (1000 nm). Therefore, the iron nanoparticles can be transferred effectively through the flow of most solutions. (Zhang 2003, 323-324.)

The specific surface area of iron in nanoscale dramatically increases because of their extra small size, resulting in enhanced surface reactivity of which could be up to 30 times higher remediation rate than 325 mesh iron powder (Yuvakkumar et al. 2011, 1771). Plus, the nano-size helps the material in water slurry be easily injected under pressure into polluted areas.

The nZVI appears to have core-shell architecture: zerovalent iron resides in the core, while outer layer contains of oxides and hydroxides forme from the shell due to oxidation on the iron surface. The core including metallic iron is in charge of contaminant removal as when it reacts and oxidizes in aqueous environment, reactants e.g. Fe (II), H/H_2, iron hydroxides and oxides are generated. (Pathakoti, Manjunath & Hwang 2019, 896.)

However, the iron is pyrophoric, which indicates its fast reactivity especially regarding to water and oxygen. This disadvantage is much greater in the case of iron nanoparticles since they quickly oxidize in the atmosphere, which limits the applications where involve water and oxygen as well as options for material preservation (Huber 2005, 484). This difficulty is the same issue that current nZVI synthetic methods are all struggling.

1.2 Synthesis of Iron Nanoparticles

Many of the earliest methods to produce clear-cut iron nanoparticles involved mercury i.e. the iron was dispersed in the chemical between 1940s and 1950s. Nonetheless, mercury-based methods have been gradually replaced with organic-solvent-based processes recently. This change seemed to concern with the confounding impacts of considerable solubility of iron in mercury along with easy removal of organic solvent, rather than the chemical's toxicity (Huber 2005, 495.) Current nZVI synthesizing procedures can be categorized as chemical, physical and mechanical methods.

1.2.1 Thermal Decomposition of Iron Pentacarbonyl

Iron pentacarbonyl ([$Fe(CO)_5$], or iron carbonyl) is decomposed in decalin at 140–160°C under an inert atmosphere to obtain iron nanoparticles, with the presence of polymer as surfactant and catalyst. The molecule is easy to decompose, but the decomposition reaction is extremely complex. The decomposition does not always result in the same reactants as different intermediate iron carbonyls and iron clusters can form and catalyse the reaction (see figure 1). These complications make the decomposing rate inconsistent and even the reacting order changes, so it is hard to regulate the size and shape of iron nanoparticles. The method somehow is still frequently used to produce iron nanomaterial, mostly owing to the ease to operate and the lack of by-products. (Huber 2005, 485 & 486.)

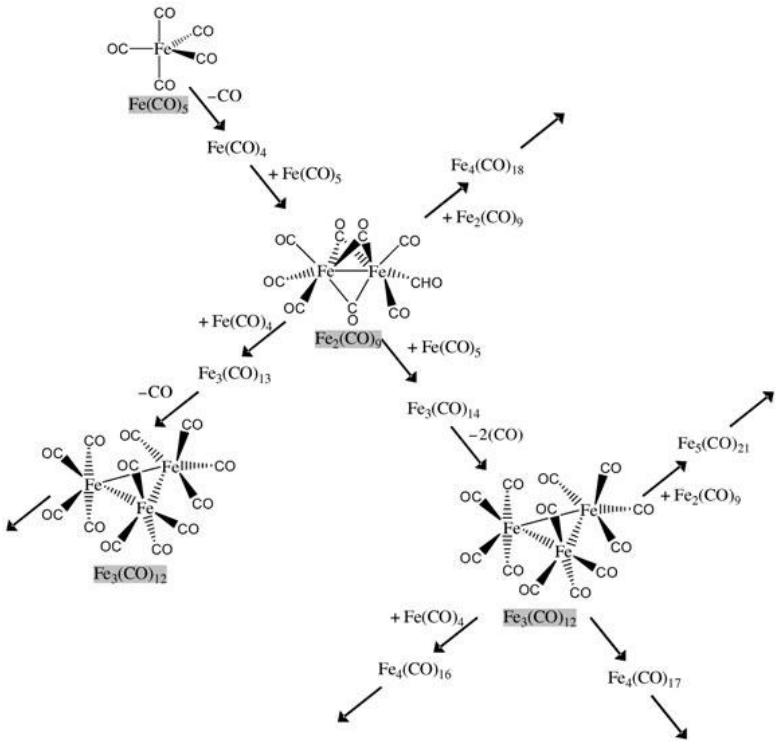

FIGURE 1. Pathways for the decomposition of $Fe(CO)_5$ (published with kind permission of Huber, 2005)

1.2.2 Sonochemical Decomposition of Iron Carbonyl

The operation of sonochemical decomposition of $Fe(CO)_5$ is as simple as thermal decomposition: acoustic cavitation is utilised to provide localised heating, causing the chemical to decompose. Neat iron carbonyl is mixed in 4M solution of decane to produce nanoscopic amorphous iron powders, which crystallize and fuse when heated above 300°C. Well-dispersed iron nanoparticles were reported to appear when polyvinylpyrrolidone (PVP) stabilizer at 0°C is added into iron carbonyl. However, it is also difficult to control the size of nanoparticles in this method. (Huber 2005, 488.)

1.2.3 Vapor Phase

Iron nanoparticles can also be synthesized by vaporizing iron into gas to separate and isolate the substance, limiting the agglomeration of the material. Iron is evaporated inside a drum wetted with a solvent and surfactant. A reservoir at the bottom of the drum contains a mixture of alkyl naphthalenes as the solvent and poly(butenylsuccinpolyamine) surfactant. The drum is rotated, mixing the solution and iron is evaporated upwards from the centre of this drum (Figure 2). The procedure has problem in controlling nanoparticle size. Plus, the surface of drum limits the amount of iron nanoparticles, so it needs to be refreshed continuously. (Huber 2005, 489 & 490.)

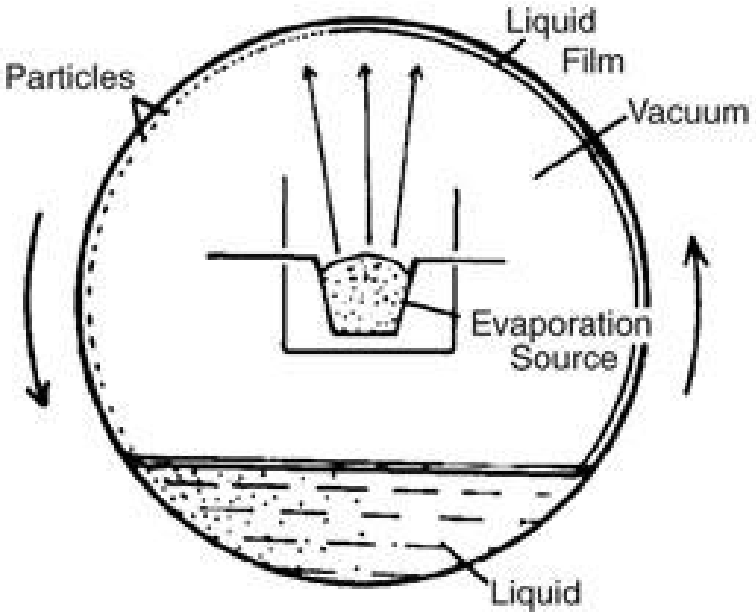

FIGURE 2. Diagram of the rotating-drum method for preparing nanoparticles (published with kind permission of Huber, 2005)

1.2.4 Mechanical Method

Iron nanoparticles can be synthesized through high-energy milling. The method seems to be unpopular in forming nanoparticles yet regarding to the economical production of large number of nanoparticles, milling is considered optimum option. It has some disadvantages as well i.e. the products are not regular in both size and shape. (Huber 2005, 491.)

1.2.5 Reduction of Iron Salt

Iron salts (either organic or inorganic) or iron oxides can be reduced to form nanoparticles. The most widely utilized example to prepare iron nanoparticles by this method is via sodium borohydride ($NaBH_4$) reduction of ferric iron (Fe(II)) or ferrous iron (Fe(III)) ions in aqueous media. This procedure is common due to its simple operation. It could be conducted safely in any laboratory with simple chemical reactants. (Sun et al. 2006, 48.)

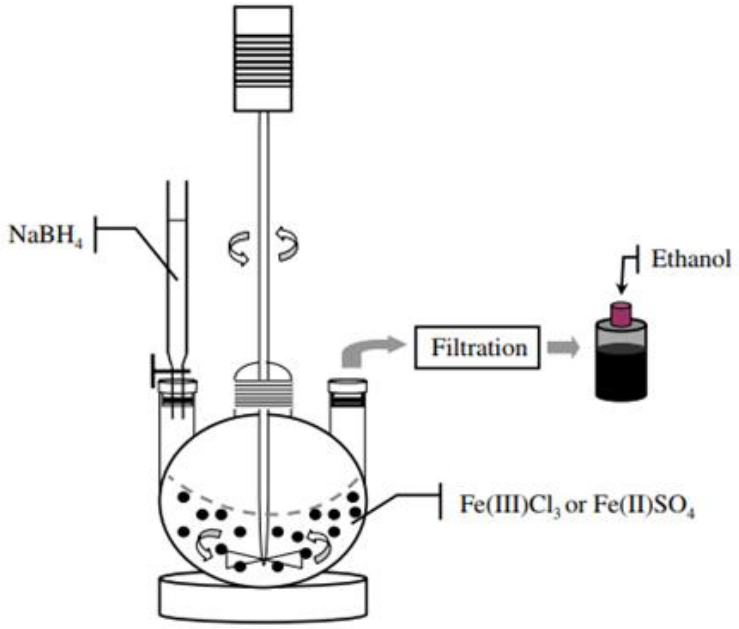

FIGURE 3. Schematic diagram of nZVI synthesis (published with kind permission of Zhang, 2006)

The reactions occur within a flask reactor that has three open necks (Figure 3). $NaBH_4$ solution is added drop by drop into iron salt solution through e.g. a

burette, while the mixture is continuously stirred by a tunable mechanical with the rate of 400 rounds/minute in a central neck throughout the whole titration. The reduction of ferric ion (Fe^{3+}) to zero-valent iron (Fe^0) can be depicted in following equation:

$$4Fe^{3+} + 3BH_4^- + 9H_2O \rightarrow 4Fe^0\downarrow + 3H_2BO_3^- + 12H^+ + 6H_2 \qquad (1)$$

The collected iron nanoparticles are washed with ethanol to prevent them from rapid oxidization. For storage, the product should be maintained a thin layer of ethanol on top. (Sun et al. 2006, 48.)

Chemical methods can produce more even-sized iron nanoparticles than physical or mechanical procedures, yet the products are unstable in atmospheric conditions. Therefore, previous studies had to perform the synthesis of nZVI in inert conditions to keep iron in its zerovalent form, by continuously directing noble gases like Ar, N_2 into the iron to keep its zerovalent form. Large consumption of noble gas causes the operation process to be uneconomical. The treatment becomes inconvenient to perform as well.

A new approach that can minimize drawbacks of all above-mentioned methods has been studied in this research i.e. a microfluidic device is applied as a reactor to conduct reduction of iron salt into nZVI.

1.3 Microfluidic Device

A microfluidic system contains channels with micrometre-scale dimensions, utilizing either active or passive control processes to manipulate small (10^{-9} to 10^{-18} litres) amounts of fluids flow within the device, which can be used as a micro optical lens, biochemical analysis appliances, fuel cells and especially, a chemical reaction vessel (Whitesides 2006, 368).

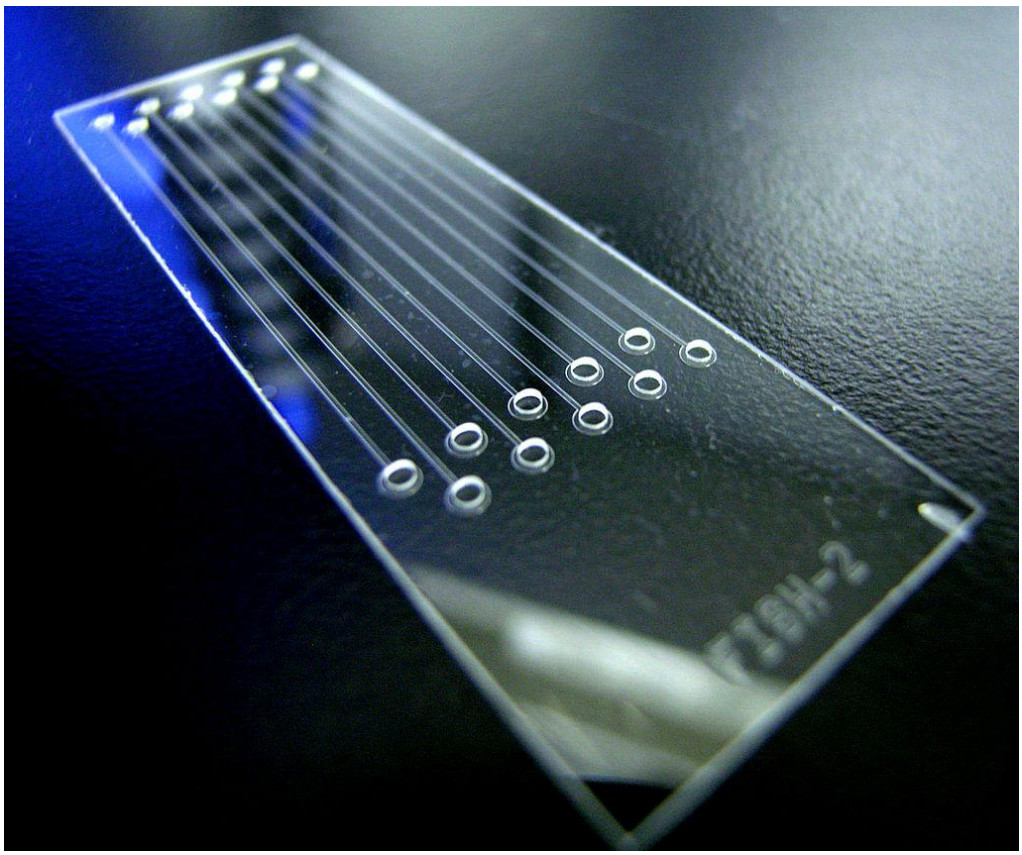

PICTURE 1. A design of microfluidic chips (Sieben 2008)

The development of microfluidics has begun since last decade. Among varieties of their applications, microfluidic chips are perhaps most developed in detecting parameters e.g. pH, ionic strength, composition or concentration for protein crystallization. The devices are also popular in bioanalyses, particularly in live imaging and cell cytometry. (Whitesides 2006, 370.) At the moment, it can be seen that the application of microfluidic devices is thriving most in the medical and biological fields. However, a microfluidic chip has huge potential in industry as well when it can replace a large system and work as a chemical reactor. There has been a number of articles related to this issue, yet the idea of using a microfluidic device as a micro reactor to produce nanomaterial has not grown as strong as it should be. Therefore, this research proposes a potential design of microfluidic reactor for nanomaterial preparation in general and nZVI in particular. The device has been under experiment several times to examine its capability. The results show promising advances: even-sized nanoparticles, compact design, decrease in manufacturing cost and the process can be simply automated by controlling the reagent solutions with micropumps, to name but a

few. Hence, the microfluidic reactor is expected to be utilized ubiquitously in the future.

1.4 Iron Nanoparticle Applications

1.4.1 Magnetic and Electrical Application

There are such many feasible utilizations of iron nanoparticle in magnetism and electricity field, and among them the largest commercial application would probably be magnetic recording media, where high coercivity is crucial. For example, advanced magnetic tapes i.e. those installed in computer backup tapes and camcorders can obtain their high capacity through the use of iron nanoparticles. (Huber 2005, 495.)

1.4.2 Biomedical Applications

Iron nanoparticle offer a wide range of advances in biomedicine as a result of its nanometric properties coupled with magnetic feature. These applications include biomedical imaging (MRI contrast improvement, molecular imaging, MPI, imaging of cell therapy, etc.), directed drug delivery, labelling and magnetic separation of biological materials, tissue engineering and hyperthermia treatment. (Silva et al. 2016, 426; Huber 2005, 497.)

1.4.3 Environmental Applications

As mentioned above, in these days, zerovalent iron nanoparticles and metal-coated iron nanoparticles have been applied extensively in wastewater treatment as well as hazardous chemical removal. Recent research has showed that the morphology coupled with structure of nZVI contribute to the eliminations of various contaminants such as chlorinated compounds (CCl_4, $CHCl_3$, CH_2Cl_2, CH_3Cl), pesticides (DDT, Lindane), organic dyes (Orange II, Chrysoidine,

Tropaeolin O, Acid Orange, Acid Red), heavy metals (Hg^{2+}, Ni^{2+}, Ag^{+}, Cd^{2+}) and so on (Yuvakkumar et al. 2011, 1771; Zhang 2003, 326; Zhang & Wang 1997, 2154-2156; Liu et al. 2005, 1338; Xu et al. 2005, 449; Alowitz & Scherer 2002, 299; Kanel et al. 2005, 1291).

What is more, the material can suspend for a sufficient period of time to create an in-situ treatment zone. That makes iron nanoparticles flexible for both in situ and ex situ remediations (Zhang 2003, 324.) In fact, since 2001, nZVI has become favoured in pilot- and field-scale applications. For example, nZVI was used to treat 44 CVOC-contaminated sites in 2009. The number of polluted areas that were remediated with nZVI kept increasing i.e. it was 59 sites in 2013 and 77 sites in 2017. These locations were in USA, Canada, some European countries and Taiwan (Phenrat & Lowry 2019, 14.)

Thanks to its versatile applicability, nZVI can be utilised in water, ground water or wastewater treatment from any sector of industry. Industries that involve a wide range of chemicals e.g. mining, plastics, paper, food and so on would release the most toxic effluents into the nature. This project decided to concentrate on the potential of iron nanomaterial for treatment of wastewater generated by textile and garment industry. Specifically, nZVI has been proved to effectively transform organic dyes such as azo dyes (Methyl Orange) and thiazine dye (Methylene Blue) into less toxic substances. These dyes hardly biodegrade and photodegrade, which could lead to reduced penetration of sunlight, eutrophication as well as interruption with receiving water ecology if they were left to accumulate in nature (Li et al. 2015, 2.) Another reason for this project to mainly contemplate treatment for effluents from textile industry is that in Vietnam where the research is taking place, the textile industry has been developing tremendously for the last five years. The industry is estimated to have a high export turnover coupled with an average growth rate of more than 13% over the years, accounting for approximately 14% of the total national exports (Tran & Tran 2018, 46). However, the treatment processes for by-products as well as disposal from the textile manufacturing are still limited, including conventional techniques with low efficiency. Thus, it is crucial that wastewater treatment involved nanotechnology with nZVI be analysed and widely applied in the industry in the near future.

2 AIMS AND SCOPE

The thesis mainly aims at designing a new model of microfluidic device and applying it as a microreactor for synthesizing zero-valent iron nanoparticles, which had been highly considered a promising adsorbent of water contaminants in recent research. The as-prepared nanomaterial was then assessed for potential in wastewater treatment, particularly in removing organic colour dyes from textile industry's effluents.

This thesis works as a short summary of the project *Preparation of zero - valent iron nanoparticles by microfluidic reactor for organic dyes treatment in industrial wastewater* supported by National Foundation for Science and Technology Development (NAFOSTED) of Vietnam under the grant No. 103.99-2018.11. In this research, the device was prepared by photolithography and soft moulding processes. The nanoparticles were studied in terms of their morphology and structure, while their capability in removing dye molecules was analysed based on the colour degradation. The factors that could affect the treatment process were considered the dosage of nZVI used and the pH conditions.

3 METHODS

3.1 Apparatus

In this work, the nanoscale iron particles were produced from reaction of sodium borohydride ($NaBH_4$) with iron (III) chloride ($FeCl_3.6H_2O$). Ethanol 92% was used for preparing those two reagents. The experiments were performed on two types of dyes, methyl orange (MO) and methylene blue (MB).

3.1.1 Microfluidic Reactor

The micro mixer is considered the most significant part of a microfluidic reactor as the design of mixer would affect the mixing efficiency. The curved or wavy micro-channel is the most common figure for micro mixer thanks to its simple design and easy control, yet the mixing efficiency is not considerably high. Previous studies have shown that a spiral model would obtain the highest mixing performance among other types through experimentation. (Ngo et al. 2020, 1.) Thus, double spiral micromixers were specifically fabricated for the microfluidic device in this work.

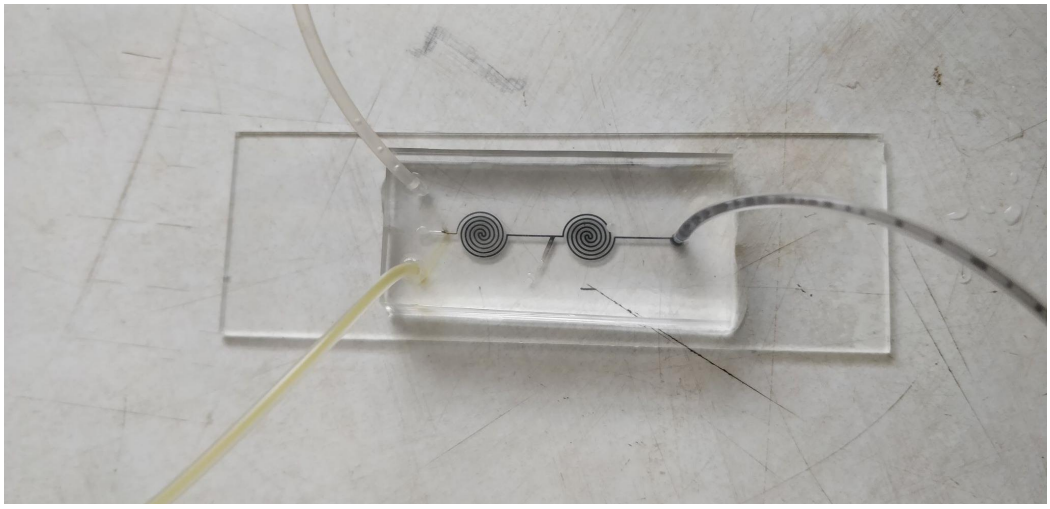

PICTURE 2. The microfluidic reactor in this experiment

3.1.2 Other equipment

The experiment system included two single syringe pumps (KDS 100 model from KD Scientific) attached to the microfluidic reactor. There were also an ultrasonic cleaner, which assisted in controlling the nanoparticle flow, a microscope connected with PC for observing the device and an air pump to spread the nanomaterial evenly within the samples throughout treatment.

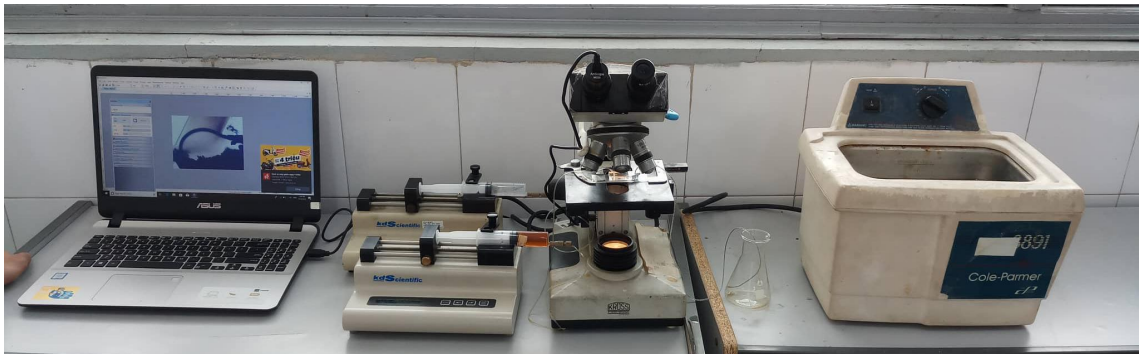

PICTURE 3. Setting up the experiment (taken by Le Nguyen)

3.2 Procedure

Poly(dimethyl-siloxane) (PDMS) was chosen to prepare the device since the material is optically transparent, biocompatible, non-flammable and low in toxicity (Dang 2011, 5 & 13). The microfluidic device was fabricated through three main phases: (1) design the film mask, (2) manufacture silicone wafer by photolithography technique and (3) fabricate the microchannel system on PDMS by soft moulding method.

The film mask was firstly drafted on AutoCAD. Some auspicious sketches were chosen to make the prototypes. The procedures for photolithography and soft lithography could be simply described in figure 4.

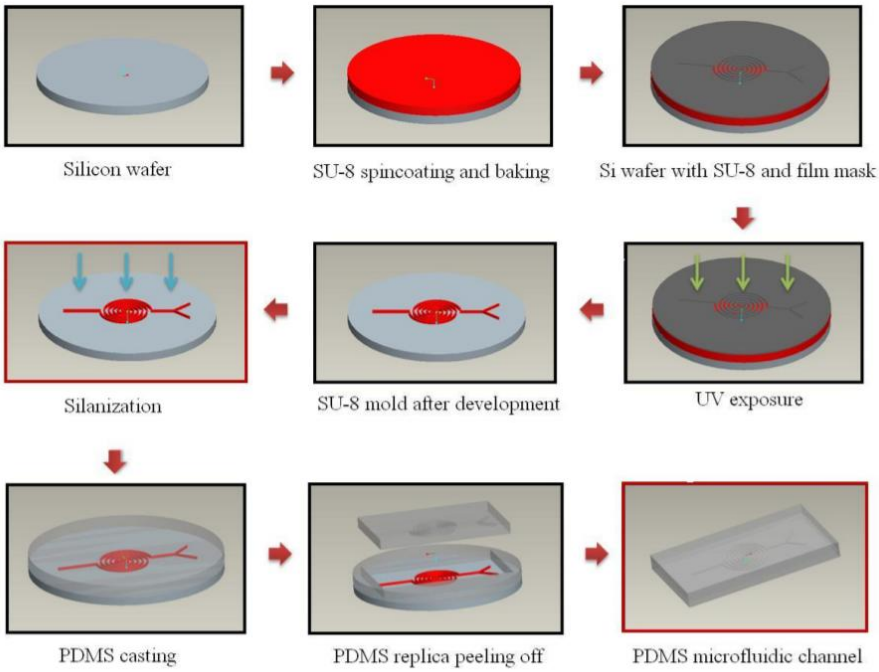

FIGURE 4. Schematic image of microfluidic device production (published with kind permission of Dang, 2011)

The flow rate for each pump was stimulated by using Computational Fluid Dynamics (CFD) software, then several trials were made to determine at which speed the flows would be consistent and the products would result in most regular size.

3.2.1 Experiment

0,54g $FeCl_3.6H_2O$ was dissolved in ethanol/water mixture of 4/1 parts in volume i.e. 24 ml ethanol + 6 ml distilled water, resulting in 0,067 M $FeCl_3$ solution. Since $NaBH_4$ was hard to dissolve in ethanol, 0,38g $NaBH_4$ was first dissolved in 50 ml of deionized water. The solution was then added with 50 ml of pure ethanol to obtain 100 ml of 0,1 M $NaBH_4$ solution.

Two solutions $FeCl_3$ and $NaBH_4$ were input into the syringe pumps that had been set up i.e. the diameters of both syringes were 20 mm and the rate was 0,1 ml/h for $NaBH_4$ and 2,0 ml/h for $FeCl_3$. Specifically, approximately 10 ml of $FeCl_3$ and 20 ml of $NaBH_4$ were taken as the exceeded borohydride was used

to accelerate the reaction. The device was then connected with two syringes through micropipes.

PICTURE 4. Setting up the pumps

When the pumps were started, the output micropipe was left in a 50 ml beaker for about 10 minutes to wait for the flow rate to become constant. The iron nanoparticles were then directed into the samples to start the treatment. During the treatment, if the nanoparticles seemed to accumulate in the output and block the transportation, the device would be put into the ultrasonic bath to clear the way. In addition, the samples were stirred with air pump from start to finish.

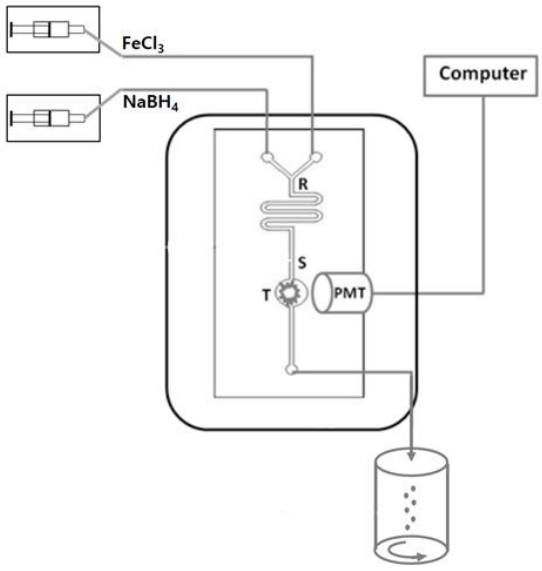

FIGURE 5. Diagram of synthesis of nZVI with microfluidic device and application in removing organic dyes

10 ml of MO 25 mg/l solution would be treated within 60 minutes using nZVI generated by microfluidic reactor in different times from 10, 20, 30 to 40 minutes. To put it simply, the nZVI was transferred into MO solution for e.g. 10 minutes then was left to be aerated for another 50 minutes. The same procedure was applied for other samples. After one hour of treatment, the samples were filtered and the collected nZVI was washed with distilled water five times, then was dried in vacuum dryer. In MB case, the process was similar, except for the treatment time. 10 ml of MB 1 mg/l would be treated in 30 minutes while nZVI was directed into the sample in 2, 4, 6, 8 and 10 minutes.

To prepare the samples with different pH, catalysts (NaOH and HCl) were added into each sample to obtain pH of 1, 3, 5, 7, 9, and 11. A pH meter and litmus papers were used to determine the if solutions reached the required pH. These samples were treated in 30 minutes with the amount of nZVI synthesized in 10 minutes.

3.3 Analysis Methods

The morphology of the as-prepared material was examined with scanning electron microscope (SEM) technique using Hitachi S-4600 model while its structure was studied with X-ray diffraction (XRD) on the X'Pert Pro device of PANAnatycal. Source of X-rays was Cu K-alpha, and the generator settings were 45 kV and 40 mA. Scans ranged from 15° – 90° 2θ with a 0,5° step size.

For the colour degradation of the samples treated with as-prepared nZVI, the ultraviolet–visible spectroscopy (UV-vis) analysis was applied by using Agilent 8453 model.

The efficiency of nZVI in removing dye molecules from the samples with different contact time could be calculated using following formula:

$$R = \frac{c_0 - c_t}{c_0} \times 100 \qquad (2)$$

In which

R is removal efficiency (%)

c_0 is the initial concentration of chemical (mg/l)

c_t is the concentration of chemical at *t* minute(s) (mg/l)

Since the concentration of chemical was directly proportional to the absorbance, the above formula could be written as:

$$\mathrm{R} = \frac{\mathrm{A}_0 - \mathrm{A}_t}{\mathrm{A}_0} \times 100 \qquad (3)$$

In which

A_0 is the absorbance of original sample at absorption peak (Au)

A_t is the absorbance of sample at *t* minute at absorption peak (Au)

The calculation for removal efficiency in terms of pH effects was similar, particularly:

$$\mathrm{R} = \frac{\mathrm{A}_0 - \mathrm{A}_i}{\mathrm{A}_0} \times 100 \qquad (4)$$

In which

A_i is the absorbance of sample with pH value *i* at absorption peak (Au)

4 RESULTS AND DISCUSSION

4.1 Design of Microfluidic Device

A number of microfluidic devices with different structures had been designed in AutoCAD and shown below.

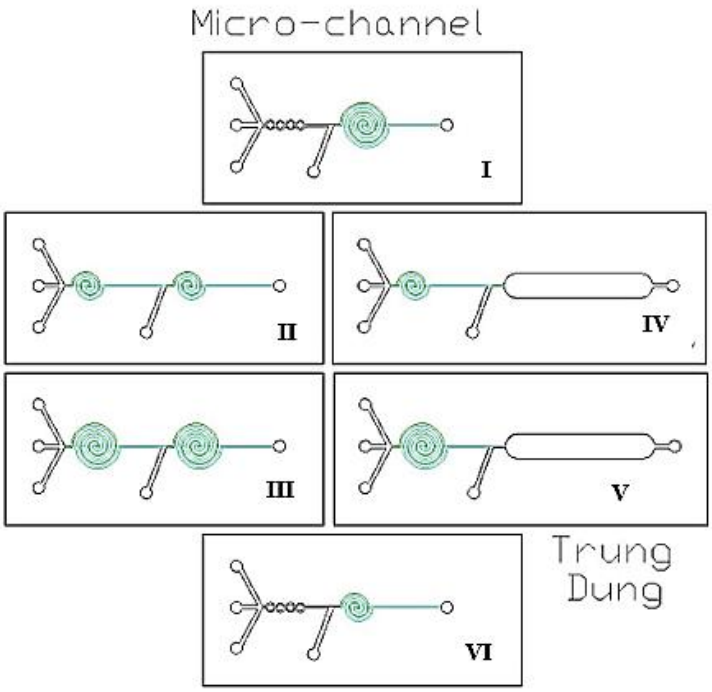

FIGURE 6. Some designs of microfluidic reactors (published with kind permission of Dang, 2018)

As it was stated, spiral microchannel was considered to have highest mixing efficiency, therefore the design III was selected as the microfluidic reactor for this research. In addition, the pumps' rates were optimized via CFD program as 0,1 ml/h for $NaBH_4$ and 2,0 ml/h for $FeCl_3$.

4.2 Properties of nZVI

When two reagents were pumped into the microfluidic device and mixed, the synthesis reaction occurred inside the reactor and could be explained via following equation:

$$2FeCl_3 + 6NaBH_4 + 18H_2O \rightarrow 2Fe^0 + 6NaCl + 6B(OH)_3 + 21H_2 \qquad (5)$$

The mixture turned into black and a great amount of H_2 evaporated, which were observed through the microscopy connected with the computer. The black products formed by chemical reactions within the device were directed into the dye samples, suspended within the solutions and only settled down after a few hours. This indicates that the nanomaterial had quite small specific weight value. These nanoparticles were also tested to be attracted to magnets, demonstrating the typical magnetism of ferromagnetic materials. The product would turn to yellow if it was left exposing to the open air for some time, implying that it was oxidized in the normal condition. In addition, when the substance was filtered and dried, a black smooth powder was gathered. The powder could be resulted from extremely small fine particles.

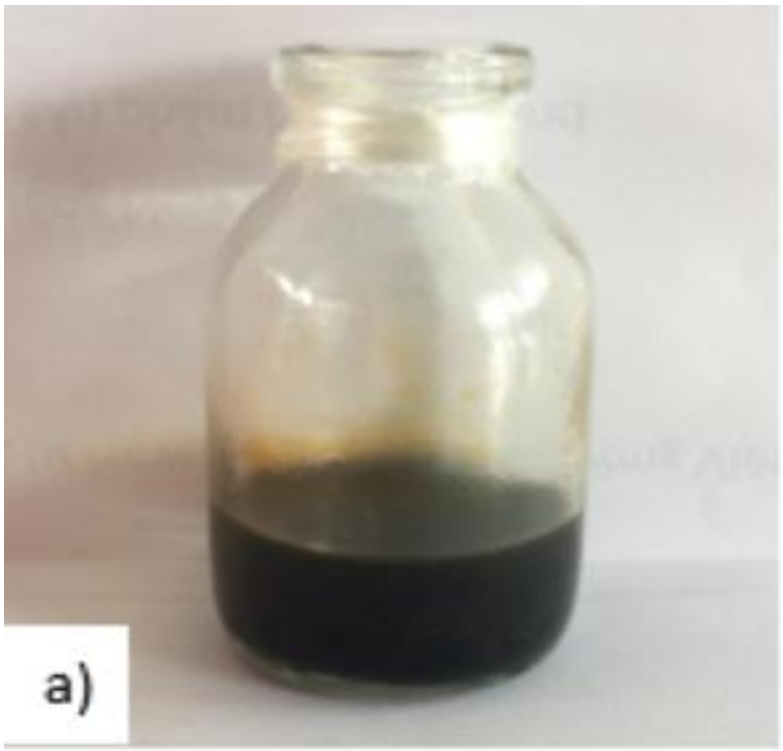

PICTURE 5. Nanomaterial collected from microfluidic synthesis (taken by Le Nguyen)

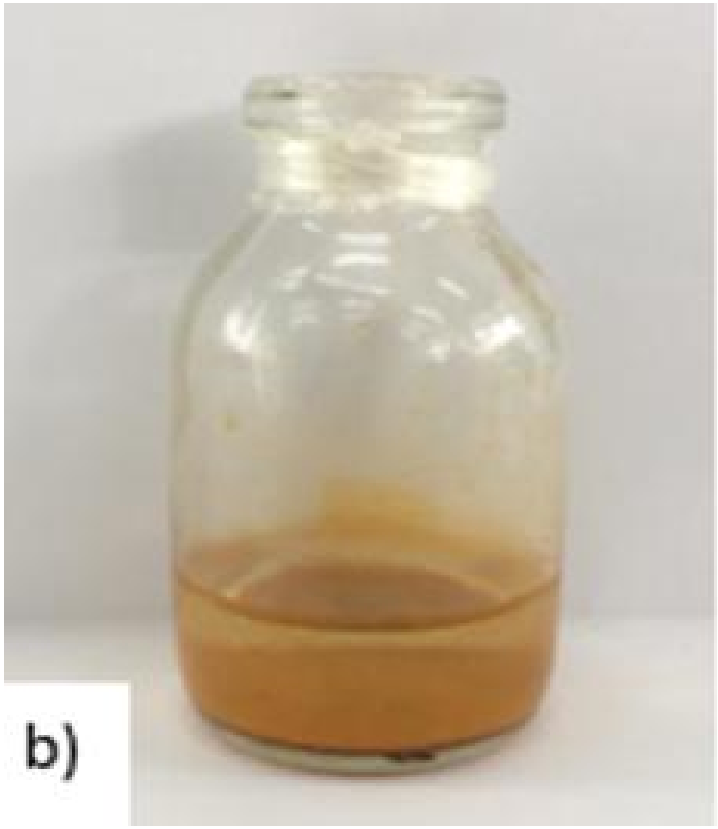

PICTURE 6. The product turned yellow after some time in the room atmosphere (taken by Le Nguyen)

4.2.1 SEM

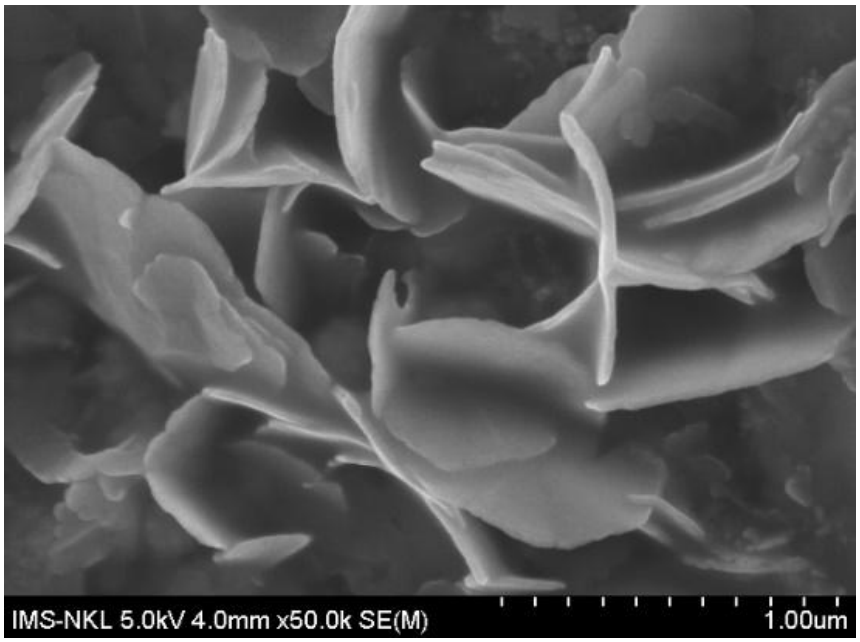

PICTURE 7. SEM image of the iron nanoparticle synthesized with microfluidic device

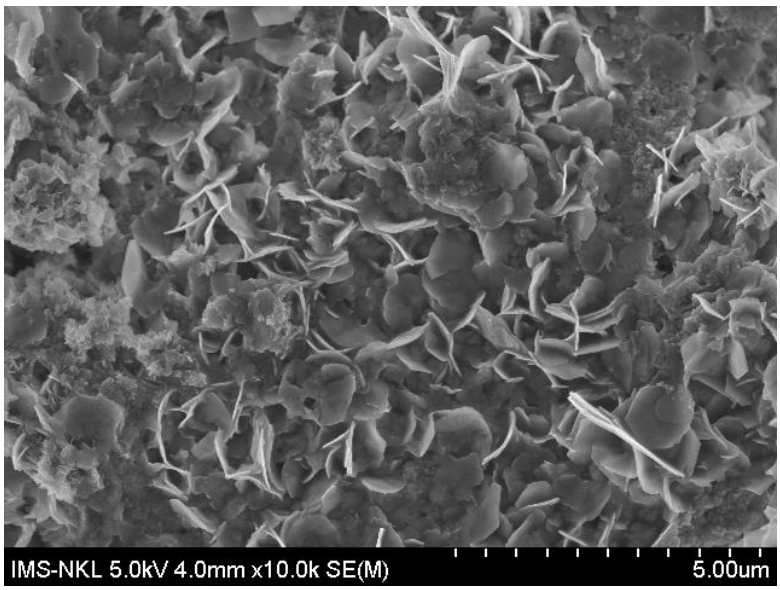

PICTURE 8. SEM image of the iron nanoparticle synthesized with microfluidic device

In picture 7 and 8, the SEM images for the collected iron nanomaterial from the microfluidic reactor were demonstrated. The products appeared in flat-sheet shape with an average thickness of 50 nm. The iron nanoparticles were densely packed on the surface layer, resulting in iron nanoclusters. This was considered a remarkable finding in this research, since previous studies or published articles indicated that the nanomaterial was in nanosphere form. Picture 9 was taken from the report of Yuvakkumar et al., which showed the SEM image of their iron nanomaterial.

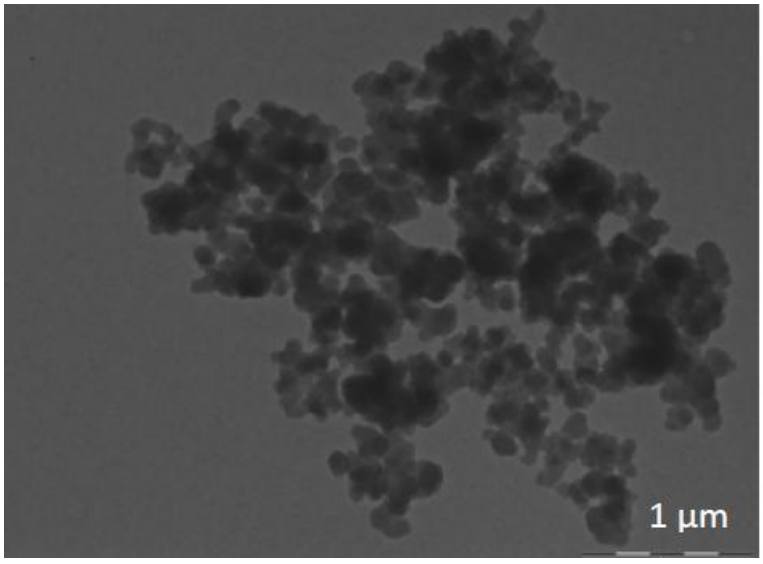

PICTURE 9. SEM image of iron nanoparticles from a previous study (published with kind permission of Rajendran, 2011)

The iron particles were seen to be in the form of nanospheres, which linked to each other and created chains. These nanoparticles had diameters of about 50-100 nm. (Yuvakkumar et al. 2011, 1773.)

In the mentioned research above, the authors conducted the nZVI synthesis by following conventional chemical method (read 1.3.5 Introduction) in ethanol medium. The similar results also appeared in the articles of Sun et al. (2006), Dozier et al. (2010) or Li et al. (2016). From these examples, it could be speculated that using a microfluidic device as reactor instead of a traditional flask filled with noble gas would produce a different shape of iron nanoparticles. This change could be explained regarding to the operation of microfluidic device. The reactions inside the device happening continuously and simultaneously, coupled with the diffusion of two reagent solutions containing Fe(III) salt and $NaBH_4$ under circumstance of high flow rate, possibly led to the formation of nanosheet. It was expected that the sheet form would perform better treatment, as the sheet shape would have larger surface area than the sphere with same volume.

After several experiments, the pumping and stirring rates for two reagent solutions within the reactor were considered to affect the formation of iron nanoparticles in terms of structure, size, uniformity of size as well as production efficiency. With different rates, the “nanosheets” appeared with different thickness. In this work, the as-prepared nZVI had average thickness of 50 nm when the system ran at 0,1 ml/h for $NaBH_4$ and 2,0 ml/h for $FeCl_3$.

4.2.2 XRD

The structure of iron nanomaterial was determined with XRD analysis and the results are shown in figure 7 below. According to the standard of ICDD Card# 06-0696, the characteristic peaks for nZVI occurred at 2Θ of 45^o and 65^o, meaning that there was nZVI in the samples. The other peaks at 2Θ of 32^o or 36^o indicated the formation of iron oxides, which were the two highest peaks. This showed that in the measured sample, iron oxides were predominantly present. The appearance of these excessive Fe oxides implied that the

preservation of samples before XRD study had difficulty in preventing oxidation, especially in atmospheric conditions. Furthermore, filtering and drying processes would mostly let the material be exposed to the air, causing the substance to oxide.

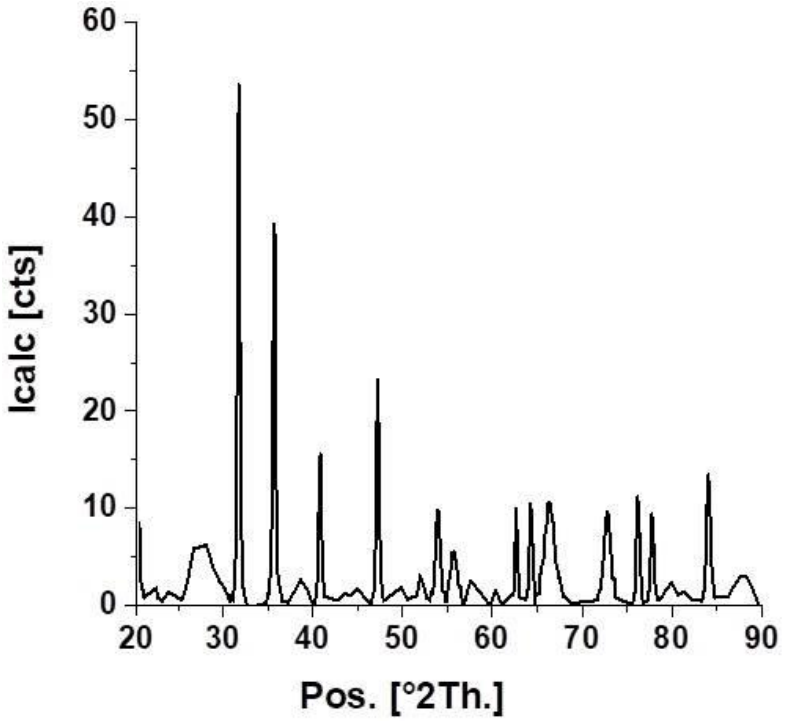

FIGURE 7. XRD spectrum of nZVI

4.3 Potential of nZVI in removing organic dyes

In this section, the UV-vis results for MO and MB samples are presented along with calculation of removal efficiency. There were two factors considered to affect the treatment i.e. the dosage of nZVI and the pH level of samples.

4.3.1 Methyl Orange

There were three chemical reaction mechanisms possibly taking place during the MO treatment with nZVI, namely coprecipitation, advanced oxidation with hydroxyl radicals formed by reaction of Fe^{0+} ions with H_2O and electrochemical reduction on the surface of these nanoparticles. The general mechanisms for

the removal of MO from samples with nZVI present as catalyst can be defined in following chemical equations (Figure 8).

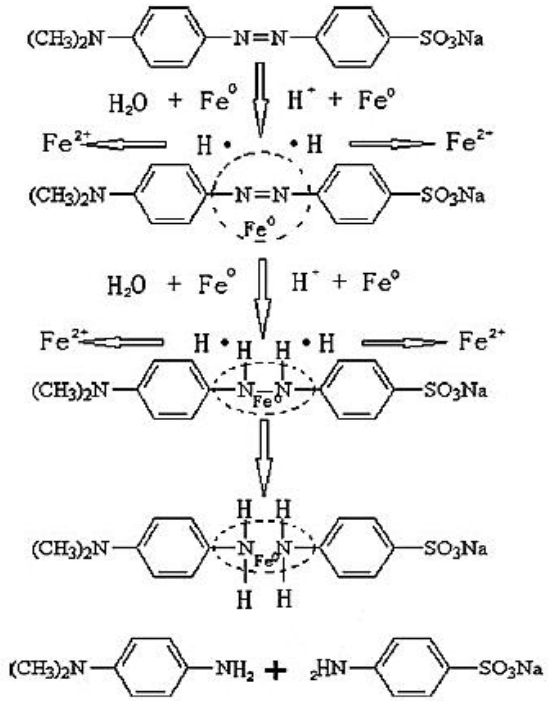

FIGURE 8. Proposed mechanism for MO treatment using nZVI (Chen et al. 2011)

To put it simply, when MO molecule was adsorbed onto the surface of nZVI, it was combined with one Fe^0. On the other hand, another Fe^0 united the previous mid-body and integrated two more radicals of H again, leading to the formation of chelate complex of Fe(II)–dye as well as breakage of the -N=N- bond. (Chen et al. 2011, 606.)

There were huge differences in colour of each sample from visual observation at first. The typical orange in initial sample gradually reduced to a relatively colourless solution after different periods of treatment time (10, 20, 30 and 40 minutes) (Picture 10).

PICTURE 10. Colour reduction in MO 25 mg/l after nZVI treatment

The UV-vis results (from wavelength of 300 nm to wavelength of 600 nm) for treating 10 ml of MO 25 mg/l solution with different amount of nZVI in 60 minutes were presented in Figure 9. The characteristic peak for MO could be clearly seen at wavelength of 464 nm. When the amount of nZVI transferred into the MO samples increased, the absorbance at peak 464 nm significantly declined i.e. from 1,75 Au to approximately 0,01 Au. The visible adsorption peak vanished due to the fact that the azo double bond was caused to open and disconnect by radicals of H generated by the reaction of nZVI nanoparticles with H_2O (Chen et al. 2011, 606). This reflected that the orange colour in original sample almost disappear after 40 minutes of feeding iron nanoparticles.

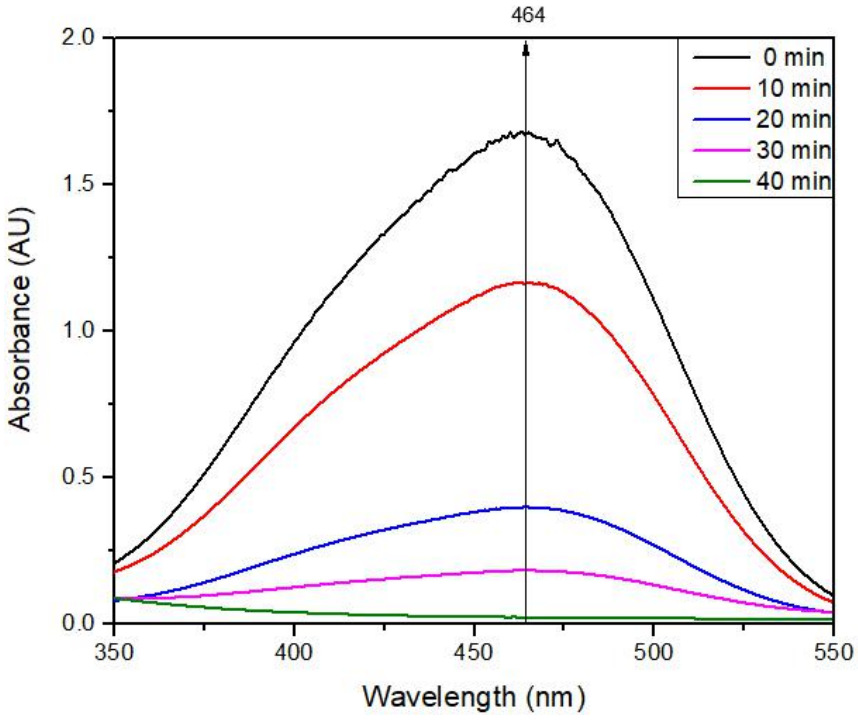

FIGURE 9. UV-Vis spectrum of MO after treatment in different times

The nZVI quantity produced in the reactor that depended on the time for sample synthesis could be calculated based on equation 5 in condition that $NaBH_4$ was used up (see Appendix 1 for detailed calculation). When the reaction time ranged from 10, 20, 30 to 40 minutes, the amount of iron nZVI gradually increased. It could be seen that the concentration of MO removed from sample correlated to the number of iron nanoparticles used during experiment, which was presented in table 1. The nZVI's efficiency in removing MO from samples could be calculated by using formula 3.

TABLE 1. The amount of nZVI proportional to MO concentration and removing efficiency

nZVI synthesis time (min)	**nZVI formed (g)**	**MO concentration after treatment (mg/l)**	**Removal efficiency (%)**
0	0	25	0
10	$3,11.10^{-5}$	17,42	30,32
20	$6,22.10^{-5}$	5,85	76,6
30	$9,33.10^{-5}$	4,93	80,3
40	$12,44.10^{-5}$	0,33	98,68

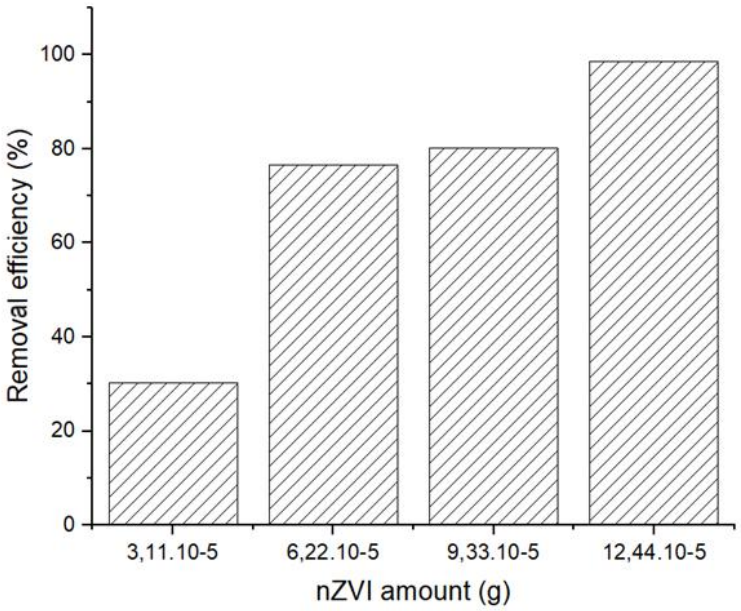

FIGURE 10. nZVI amount versus MO removing efficiency chart

The initial concentration of the sample which was 25 mg/l was denoted as 100%. After 60 minutes of treatment, the reduction in MO concentration, which indicated the solution's colour percentage, was directly proportional to the quantity of prepared iron nanoparticles. Specifically, the number of iron nanoparticles was raised after each treatment, from $3{,}11.10^{-5}$ g to $12{,}44.10^{-5}$ g, resulting in colour degradation of MO from approximately 30% to nearly 99%. The initial concentration of MO was 25 mg/l that went down to 17,42 mg/l after first trial. The concentration continued to decrease to 0,33 mg/l after 40 minutes with ca. $12{,}44.10^{-5}$ g of iron nanoparticles. Thus, it could be concluded that the more nZVI transferred into the samples, the lower the MO concentration. This could be simply understood that when more dosage of nZVI was added into the solution, the adsorbent surfaces would be increased, leading to more available sites for iron – MO complex formation (Yang et al. 2018, 4).

To evaluate how pH affected the MO treatment in MO 25 mg/l solution with iron nanoparticles, all the samples were conducted with the same nZVI amount of 31,11 µg in 10 minutes. Picture 11 shows the samples after being modified to obtain equivalent pH levels.

PICTURE 11. MO samples with different pH (taken by Le Nguyen)

The colour in each sample remarkably changed after being treated with nZVI, especially with pH 1, the solution became relatively transparent (Picture 12). This outcome proved that pH did have impacts on the treatment process with nZVI.

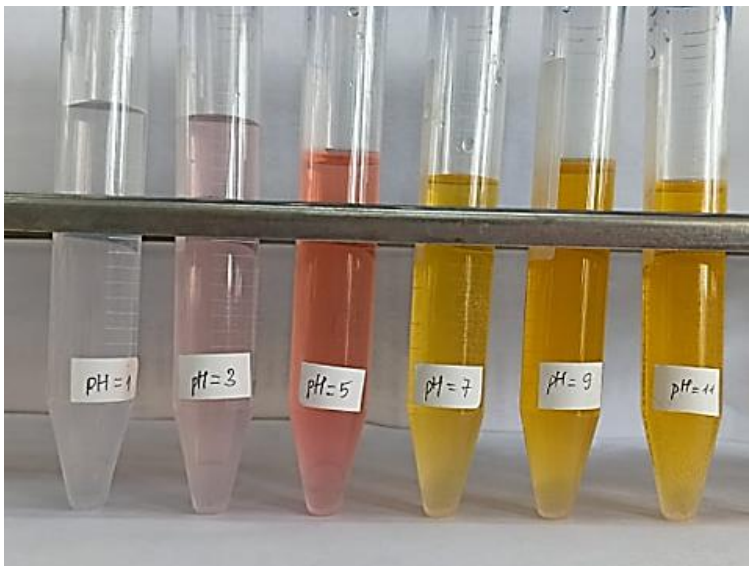

PICTURE 12. MO samples with different pH after treatment (taken by Le Nguyen)

These samples were analysed with UV-vis. The results were quite similar with figure 9 i.e. the characteristic peak for MO was at wavelength of 464 nm, except for the pH 5 solution, implying that the sample could have turned into a different substance. The absorbance went down when the pH values decreased, and it could be seen that when pH varied between 1 and 3, there was no peak at wavelength of 464 nm. At pH 1, the absorbance could be considered 0.

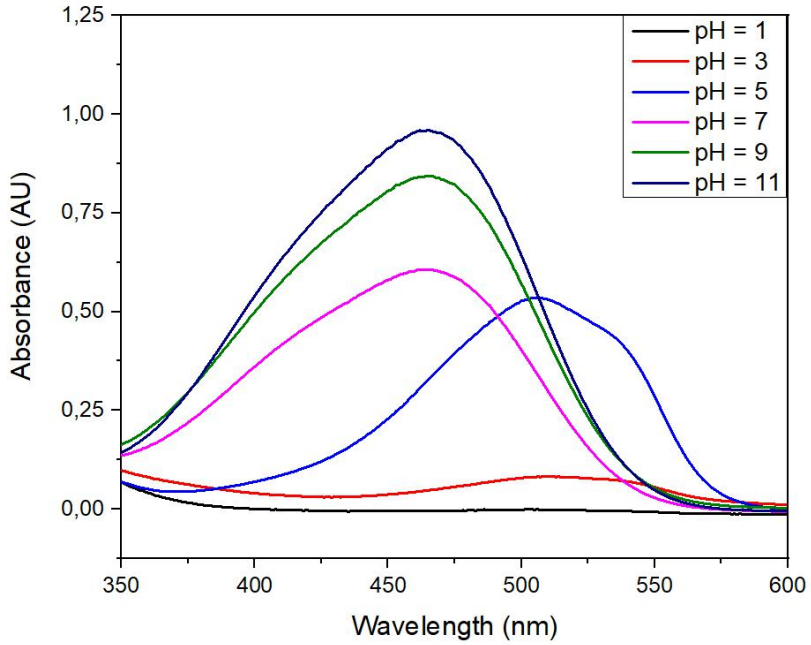

FIGURE 11. UV-vis spectrum of MO 25 mg/l solutions with different pH

The removal efficiency of nZVI could be calculated with formula 4 based on the absorbance data from UV-vis result and are shown in table 2 along with figure 12.

TABLE 2. MO concentration in each sample after treatment

pH	MO concentration after treatment (mg/l)	Removal efficiency (%)
1	7,5	70
3	1,25	95
5	8,36	66,56
7	9,48	62,08
9	13,19	47,24
11	15,02	39,92

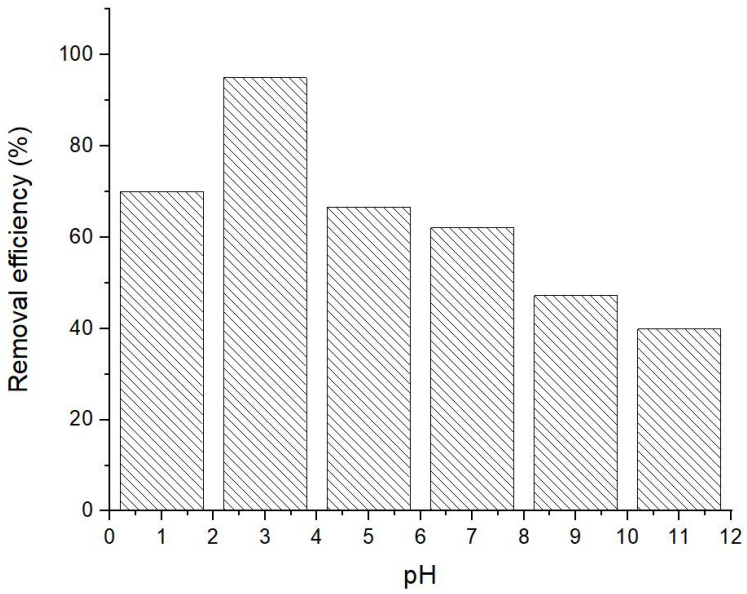

FIGURE 12. pH level versus efficiency in removing MO chart

The removal of MO gradually decreased when the pH rose from 3 to 11 and at pH 3 the efficiency reached the highest, 95%. This could be due to the ionization on the surface of nZVI and the deprotonation of MO, which resulted in favourable adsorption of MO onto iron oxide on the surface of iron nanoparticles. Specifically, MO was negatively charged as it was an azo dye with a sulphuric group so at low pH condition, Fe (II) – MO complex was formed in the presence of H^+, leading to the reduction of MO. When pH increased, hydroxide

precipitation was slowly generated and obscured the surfaces of nZVI. Thus, the MO removal started to slow down (Chen et al. 2011, 604.) This result also supported the idea that higher concentration of nZVI would obtain higher MO reduction in previous experiment.

Overall, it could be concluded that nZVI could perform treatment best at pH 1 to 3 (acidic condition) in accordance with previous published reports on application of iron nanoparticles in wastewater treatment, particularly elimination of MO.

4.3.2 Methylene Blue

The removing process of MB could occur according to four major mechanisms: reduction, degradation, adsorption and precipitation. Figure 13 presents how MB is possibly eliminated by nZVI.

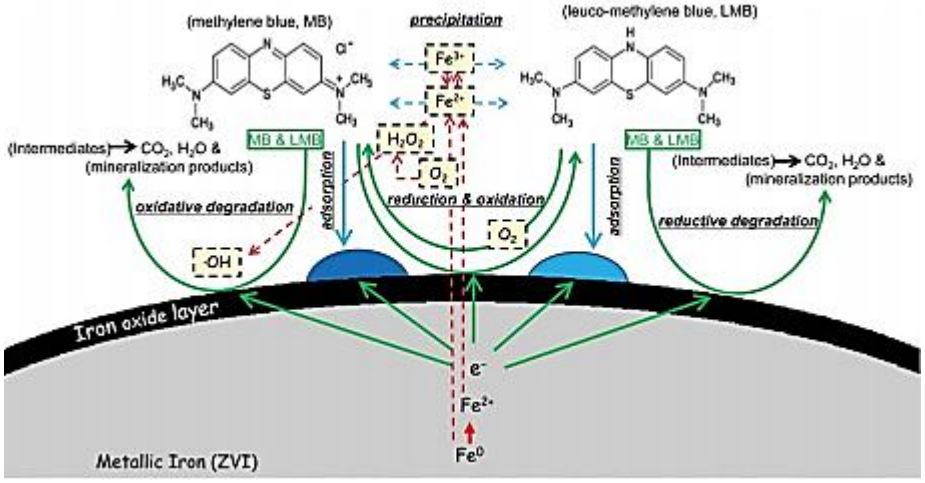

FIGURE 13. MB removing mechanisms (published with kind permission of Kawase, 2015)

nZVI reduces MB molecules to colourless leuco-methylene blue (LMB), but the reduction is unstable so LMB can be readily oxidized back to MB (Sun et al. 2015, 1058). In this study, it had been observed that the samples after treatment could still recolour if it was kept being aerated. Therefore, the transparent solution after reduction might mostly contain LMB. This is also considered the most major mechanism for MB decolourization among four mechanisms.

In degradation, the MB molecules are firstly adsorbed onto the nZVI surface. Then the reductive cleavage of the chromophores in MB, C_4H_5NS, occurs due to H atoms generated by nZVI reacting with H_2O and causes the decolourization and mineralization of MB later on (Sun et al. 2015, 1058.)

Adsorption happens in MB removing process mainly because complexes of MB and intermediates with Fe (II) and Fe (III) oxides/hydroxides are adsorbed on the surface of nZVI during its corrosion (Sun et al. 2015, 1059).

Loss of colour in MB solution might also involve precipitation i.e. MB and the intermediates along with iron (II) and iron (III) oxides/ hydroxides precipitate during the reaction and possibly on the nZVI surface as well (Sun et al. 2015, 1059).

The experiments showed some positive results found in MB treatment with nZVI, just like with MO. The initial samples, MB 1 mg/l solution, after different periods of reaction had considerable degradation in colour, which could be visually observed firstly (picture 13).

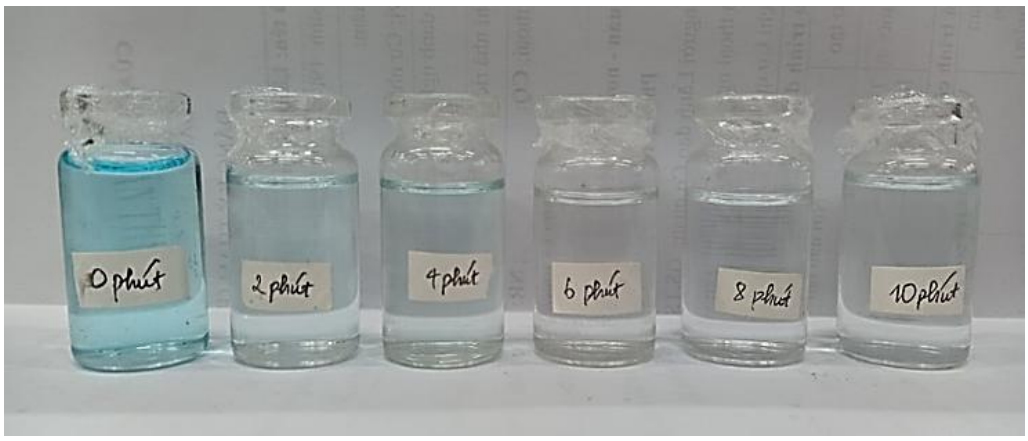

PICTURE 13. Colour degradation in MB 1 mg/l after treatment (taken by Le Nguyen)

From 6-min sample to 10-min sample, it could be seen that the typical blue colour almost vanished, indicating a reduction in MB molecules. The results would be analysed further through UV-vis data below. The absorption peak for MB was at wavelength of 665 nm. The scheme shared similarities with that of MO. Particularly, the absorbance at peak 665 nm substantially decreased from

ca. 0,16 Au to 0,01 Au when the time of treatment or the amount of nZVI increased.

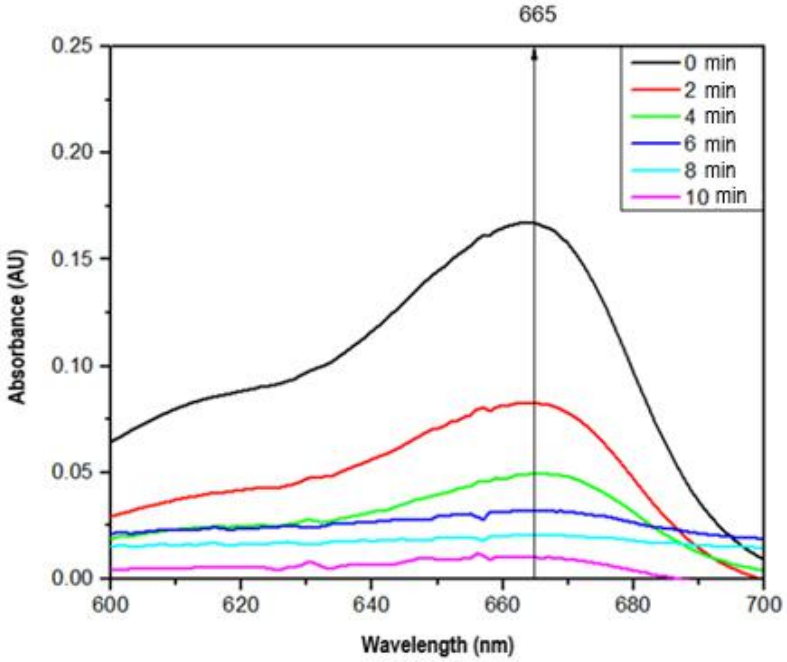

FIGURE 14. UV-vis spectrum for MB treatment in different times

The calculation result of the amount of nZVI used for each time of treatment as well as the equivalent MB concentrations are demonstrated in table 3. In addition, the impact of nZVI dosage on the removal of MB could be clearly seen in figure 15.

TABLE 3. The amount of nZVI proportional to MB concentration and removal efficiency

Time of synthesis (minute)	**nZVI formed (g)**	**MB concentration (mg/l)**	**Removal efficiency (%)**
0	0	1	0
2	$6{,}22.10^{-6}$	0,4952	50,48
4	$12{,}4.10^{-6}$	0,292	70,8
6	$18{,}6.10^{-6}$	0,192	80,8
8	$24{,}8.10^{-6}$	0,124	87,6
10	$31{,}1.10^{-6}$	0,061	93,9

If the initial concentration, 1 mg/l, was regarded as 100%, the concentrations left in solutions after every time of reaction sequentially declined, implying that more nZVI reduced more colour percentage. The efficiency could reach to 94% at 10 minutes of synthesis, with $31{,}1.10^{-6}$ g of nZVI produced. Consequently, the MB concentration went down from 1 mg/l to 0,061 mg/l. However, the rate of reduction seemed to fluctuate inconsistently. For instance, only after preparing nZVI for 2 minutes and aerating the sample, half of the MB concentration could be removed. The treatment process yet started to slow down e.g. from 6 minutes to 8 minutes only 0,068 mg of MB was eliminated, until 10 minutes just more than 90% of MB was removed. This issue was also observed in MO experiment, which could be related to the equilibrium condition and saturation of nZVI. Hamdy et al. (2018) had discovered that in early stage of adsorption, there was great number of vacant active sites for the MB reaction, so MB molecules were rapidly entrapped and removed. However, after 30 minutes of treatment, the efficiency of removal reached to around 97% then remained unchanged. This experiment could also experience the same, leading to a question whether the removal efficiency could reach to 100%.

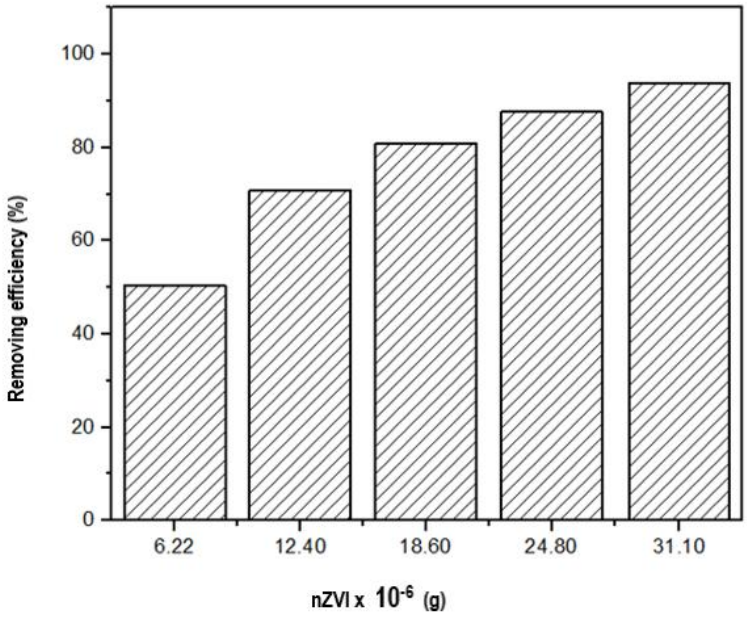

FIGURE 15. Relationship between nZVI amount and efficiency in removing MB

From all data above, it could be concluded that the higher concentration of iron nanomaterial in the samples, the lower concentration of MB.

MB was also under experiment of pH effect regarding to nZVI's decolourization. The colour in all samples had tremendously changed after the treatment. The colour degradation seemed to increase when the pH of solutions increased. Particularly, the samples with pH of 7 to 11 could be considered colourless with visual observation, while the samples with pH 1 to 5 showed light colour. The pH 1 and 5 samples somehow changed to a light greenish solution.

PICTURE 14. MB samples with different pH before nZVI treatment (taken by Le Nguyen)

PICTURE 15. MB samples with different pH after nZVI treatment (taken by Le Nguyen)

In another experiment which used silver nanoparticles to remove MB molecules had shown that the initial deep blue of MB solution changed into a light blue, then the light blue changed into light green before turning colourless (Vanaja et al. 2014, 6). Thus, it was possible that the sample with pH 1 and 5 almost reached to the transparent stage like other samples from pH 7 to 11.

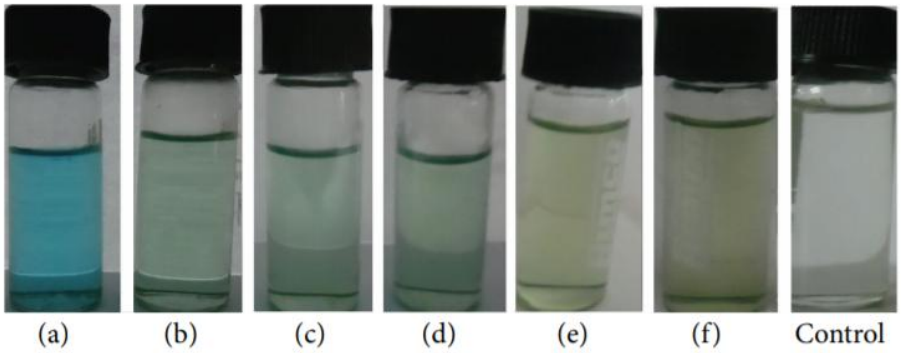

PICTURE 16. Colour changing process of MB with silver nanoparticles (Vanaja et al. 2014, available via license Creative Commons Attribution 3.0 Unported)

The detail of MB reduction could be analysed from UV-vis spectrum. At wavelength of 665 nm which was the absorption peak for MB, the sample with pH 3 whose colour was the deepest had highest absorbance, approximately 0,1 Au. The absorbance decreased when the pH values increased, except for sample with pH 1. This solution had two peaks within the range from 550 nm to 850 nm, of which the higher peak at wavelength of 750 nm could indicate a different substance other than MB. The absorbance of pH 1 sample at wavelength of 665 nm was around 0,06 Au, lower than that of pH 3 sample. Sample with pH 11 showed no peak at this range but a slight declining slope.

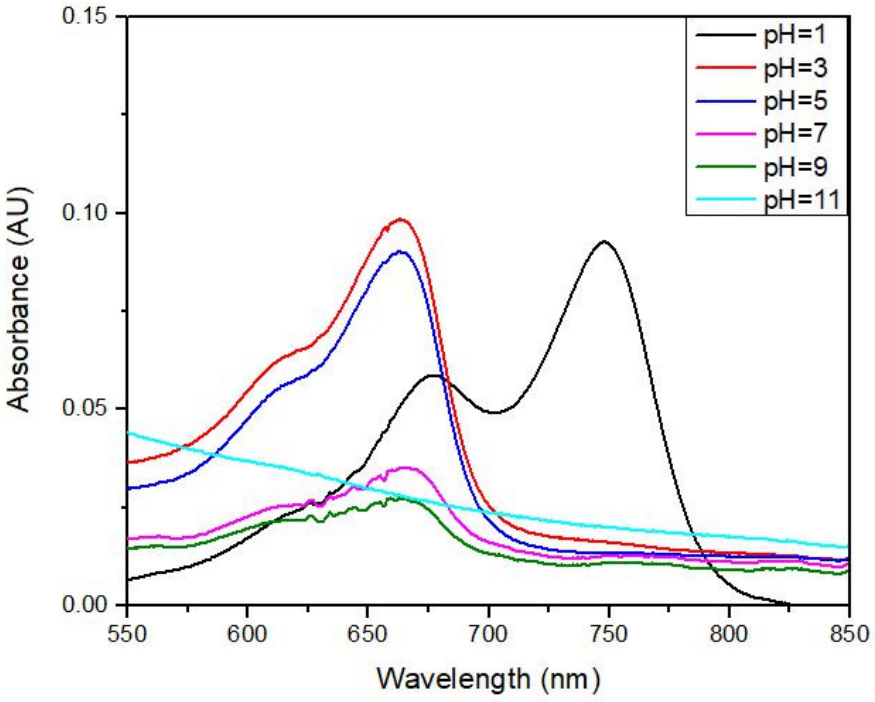

FIGURE 16. UV-vis spectrum for MB with different pH after treatment

The data for removal efficiency of nZVI related to pH impacts in MB case had been calculated and summarized in table 4.

TABLE 4. MB concentration and removal efficiency for samples with different pH

pH	MB concentration after treatment (mg/l)	Removal efficiency (%)
1	0,1868	81,32
3	0,5874	41,26
5	0,5349	46,51
7	0,2101	78,99
9	0,1633	83,67
11	0,1660	83,40

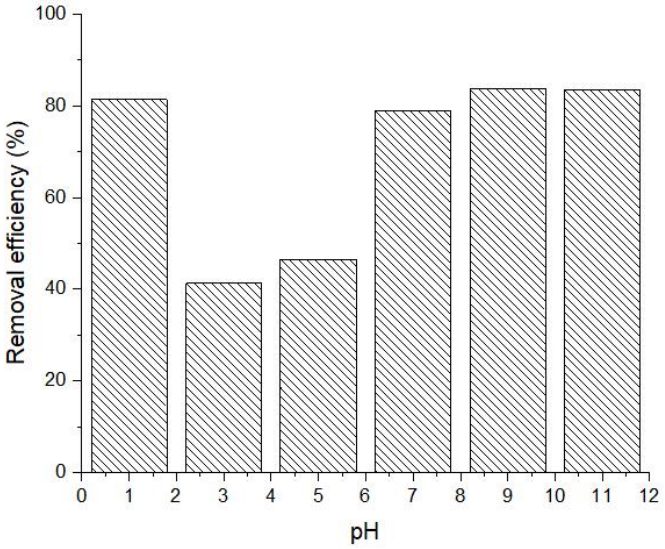

FIGURE 17. Relationship between pH and removal efficiency in MB case

The data showed that at pH 1 the concentration of MB was rapidly reduced to more than 80%. The efficiency dropped by half at pH 3 but then increased to 79% at pH 7. The efficiency stayed around 80% or more from pH 9 onwards. The great removal efficiency found at pH 1 was probably due to various iron oxides released on the nZVI surface in an acidic condition, leading to many active sites available for MB reactions. However, excessive H^+ could also compete with MB cations to reserve an adsorption site, resulting in an electrostatic repulsion. Therefore, the removal efficiency from pH 3 to 5 quickly

decreased. When the condition became more alkalic, the efficiency went up thanks to the increase in OH^- that formed an electrostatic attraction and complexes with MB molecules. A slight decline in removal efficiency appeared when pH kept rising from 9 to 11, which probably because ferrous iron and ferric iron precipitated as iron oxides/hydroxides when corrosion/hydrolysis of Fe^0 occurred in basic solution. These products could blanket the nZVI's surface and restrain the MB reduction. (Hamdy et al. 2018, 371; Singh et al. 2018, 6.)

From these data coupled with findings from previous research, it could be concluded that the removal of MB with nZVI worked best in neutral or weak basic condition (from pH 7 to 9). Yet, Fan et al. (2009) discovered that extremely acidic or basic environment caused poor performance of ZVI nanoparticles, which somehow contradicted with the result in this work (pH 1 and 11 also showed good removal efficiency). Thus, the experiments indeed need further working on.

4.4 Limitations and future improvement

The microfluidic reactor required no noble gas to prevent iron from oxidizing during the synthesis, yet the oxidization would still remain an unsolved issue in preservation process. The appearance of oxides could disrupt the study of morphology and structure of nZVI, which had been analysed in XRD result. To cease the problem, the nZVI needed to be filtered and dried in inert atmosphere as well, which was quite time-consuming and costly at that point. However, the research would propose appropriate solutions in the following stages.

A conspicuous issue appeared in analysis process was the calculation method of nZVI used dosage during treatment. The results were from theoretical measurement and the pumps' efficiency was assumed as 100%, which certainly could not happen in real experiment. In fact, the theoretical data showed that the amount of synthesized nZVI in given time was extremely small, and the practical results were expected to also be around that range. Therefore, traditional method like weighing after filtering and drying was not plausible. The research considered to apply atomic absorption spectroscopy (AAS) or

inductively coupled plasma mass spectrometry (ICP-MS) analyses in determining the nZVI concentration in sample solution. However, they were not conducted in the early stage due to lack of equipment and investment, but the project had already planned to apply in further work.

The fact that the microfluidic device needed an ultrasonic bath to reduce the accumulation of nZVI when flowing out indicates an improvement in reactor's design. It has the highest mixing rate, but it also needs to ensure the consistency of the flow in order to achieve greatest synthesis efficiency.

The project would also concentrate on measuring specific surface area of nZVI by using BET (Brunauer, Emmett and Teller) method later on. The number of organic compounds present in the solutions, which is a key indicator for the iron nanomaterial's capability in eliminating organic dyes, would be examined through total organic carbon (TOC) in the near future. Through TOC results, the removing mechanisms of nZVI in both cases could be further investigated and compared with prior study.

5 CONCLUSION

The research had designed and manufactured a microfluidic device that worked as a micro reactor for nZVI formation. The micro device synthesized a black product whose morphology and structure had been determined to own characteristics of nZVI. Furthermore, the nanoparticles collected from microfluidic reactor were actually “nanosheets” with average thickness of 50 nm. The sheet form would be further analysed in next work and compared with previous research to find any improvement compared with the sphere form.

The nZVI prepared by microfluidic reactor showed promising outcomes in decolourization of dye solutions. The amount of nZVI was considered directly proportional to the removal efficiency i.e. more dosage of nZVI in dye solutions would reduce more dye molecules, which could be up to more than 90% in both cases. On the other hand, the pH factor affected differently in different chemicals. MO was removed by nZVI most effectively in acidic condition, while it was neutral and weak basic conditions for MB. For either case, the removal efficiency was quite great, above 80%.

Overall, the early stage of this project had achieved some positive results, yet there were still some limitations that caused errors during experiments and analyses, leaving a number of unsolved issues. In the following phases, the project planned to focus on completing the most ultimate design of microfluidic reactor, investigating the reaction mechanisms that occur when nZVI decolourizes the organic dye solutions while measuring the actual nZVI concentration in samples. What is more, the project also tries switching to green chemicals such as extraction from Syzygium Nervosum leaves for reagents, as the by-products of $NaBH_4$ could cause problems if being released to the environment.

REFERENCES

Alowitz, M.J. & Scherer, M.M. (2002). Kinetics of Nitrate, Nitrite, and Cr(VI) Reduction by Iron Metal. *Environmental Science Technology, Volume 36, Issue 3*, 299-306.

Chen, Z-X., Jin, X-Y., Chen, Z., Megharaj, M. & Naidu, R. (2011). Removal of methyl orange from aqueous solution using bentonite-supported nanoscale zero-valent iron. *Journal of Colloid and Interface Science, Volume 363*, 601–607.

Dang, T.D. (2011). Fabrication of Microfluidic Devices using Microcasting for Laser Scanning and Microparticle Preparation. The Graduate School Kyungpook National University. Doctoral Thesis.

Dozier, D., Palchoudhury, S. & Bao, Y. (2010). Synthesis of Iron Oxide Nanoparticles with Biological Coatings. JOSHUA 7.

El Saliby, I.J., Shon, H.K., Kandasamy, J. & Vigneswaran, S. (2008). Nanotechnology for Wastewater Treatment: In Brief. *Encyclopedia of Life Support System (EOLSS), Volume 7,* 1-15.

Fan, J., Guo, Y., Wang, J. & Fan, M. (2009). Rapid decolorization of azo dye methyl orange in aqueous solution by nanoscale zerovalent iron particles. *Journal of Hazardous Materials*, *Volume 166, Issue 2–3*, 904–910.

Hamdy, A., Mostafa, M.K. & Nasr, M. (2018). Zero-valent iron nanoparticles for methylene blue removal from aqueous solutions and textile wastewater treatment, with cost estimation. *Water Science & Technology, Volume 78, Issue 2*, 367–378.

Huber, D.L. (2005). Synthesis, Properties, and Applications of Iron Nanoparticles. *Small, Volume 1, No.5*, 482 –501.

Kanel, S.K., Manning, B., Charlet, L. & Choi, H. (2005). Removal of Arsenic(III) from Groundwater by Nanoscale Zero-Valent Iron. *Environmental Science Technology, Volume 39, Issue 5*, 1291-1298.

Li, R., Yu, J., Shah, A., Dong, X., Li, X., Yu, H., Quan, X. & Jung, Y. (2015). Novel in situ Synthesized Fe@C Magnetic Nanocapsules Used as Adsorbent for Removal of Organic Dyes and Its Recycling. *NANO: Brief Reports and Reviews, Volume 11*, 1-12.

Liu, Y., Majetich, S., Tilton, R., Sholl, D. & Lowry, G. (2005). TCE Dechlorination Rates, Pathways, and Efficiency of Nanoscale Iron Particles with Different Properties. *Environmental science & technology, Volume 39, 1338-45.*

Ngo, I.L., Lai, T.K., Choi, H.J., Le, H.T.T., Kim, G.M. & Dang, T.D. (2020). A study on mixing performance of dean flows through spiral micro-channel under various effects. *Physics of Fluids, Volume 32, 022004*, 1-8.

Pathakoti, K., Manjunath, M. & Hwang, H-M. (2018). Handbook of Nanomaterials for Industrial Applications. Chapter 48: Nanotechnology Applications for Environmental Industry. 1st edition. Amsterdam: Elsevier.

Phenrat, T. & Lowry, G.V. (2019). Nanoscale Zerovalent Iron Particles for Environmental Restoration: From Fundamental Science to Field Scale Engineering Applications. Switzerland: Springer International Publishing AG, part of Springer Nature.

Sieben, V. J. 2008. FISH microfluidic chip (version 2). University of Alberta. Read on 28.04.2020. https://commons.wikimedia.org/w/index.php?title=Special:Search&limit=250&offset=20&profile=default&search=microfluidic+chip&advancedSearch-current={}&ns0=1&ns6=1&ns12=1&ns14=1&ns100=1&ns106=1#/media/File:FISHchip.jpg

Silva, A.K.A., Espinosa, A., Kolosnjaj-Tabi, J., Wilhelm, C. & Gazeau, F. (2016). Iron Oxides: From Nature to Applications. Part III Applications: Medical Applications of Iron Oxide Nanoparticles. United States: John Wiley & Sons.

Singh, J., Chang, Y-Y., Koduru, J.D. & Yang, J-K. (2018). Potential degradation of methylene blue (MB) by nano-metallic particles: A kinetic study and possible mechanism of MB degradation. *Environmental Engineering Research, Volume 23, Issue 1*, 1-9.

Sun, X., Kurokawa, T., Suzuki, M., Takagi, M. & Kawase, Y. (2015). Removal of cationic dye methylene blue by zerovalent iron: Effects of pH and dissolved oxygen on removal mechanisms. *Journal of Environmental Science and Health, Part A, Volume 50, Issue 10*, 1057-1071.

Sun, Y-P., Li, X-Q., Cao, J., Zhang, W-X. & Wang, H.P. (2006). Characterization of zero-valent iron nanoparticles. *Advances in Colloid and Interface Science, Volume 120*, 47–56.

Tran, T.B.N. & Tran, T.P.T. (2018). Vietnam's textile and garment industry: an overview. *Journal Business & IT, ISSN 2570-7434*, 45-53.

Vanaja, M., Paulkumar, K., Baburaja, M., Rajeshkumar, S., Gnanajobitha, G., Malarkodi, C., Sivakavinesan, M. & Annadurai, G. (2014). Degradation of Methylene Blue Using Biologically Synthesized Silver Nanoparticles. *Bioinorganic Chemistry and Applications, Volume 2014*, 1-8.

Wang, C-B. & Zhang, W-X. (1997). Synthesizing Nanoscale Iron Particles for Rapid and Complete Dechlorination of TCE and PCBs. *Environmental Science Technology, Volume 31*, 2154-2156.

Whitesides, G.M. (2006). The origins and the future of microfluidics. *Nature, Volume 442*, 368-373.

Xu, J., Dozier, A. & Bhattacharyya, D. (2005). Synthesis of Nanoscale Bimetallic Particles in Polyelectrolyte Membrane Matrix for Reductive Transformation of

Halogenated Organic Compounds. *Journal of Nanoparticle Research, Volume 7*, 449-467.

Yang, L., Gao, J., Liu, Y., Zhang, Z., Zou, M., Liao, Q. & Shang, J. (2018). Removal of Methyl Orange from Water Using Sulfur-Modified nZVI Supported on Biochar Composite. Switzerland: Springer International Publishing AG, part of Springer Nature.

Yuvakkumara, R., Elangoa, V., Rajendrana, V. & Kannan, N. (2011). Preparation and Characterization of Zero Valent Iron Nanoparticles. *Digest Journal of Nanomaterials and Biostructures, Volume 6, No.4,* 1771-1776.

Zhang, W-X. (2003). Nanoscale iron particles for environmental remediation: An overview. *Journal of Nanoparticle Research, Volume 5*, 323–332.

APPENDICES

Appendix 1. Theoretical calculation of nZVI amount

The mole of $NaBH_4$ flowing in 1h was calculated as following:

$$\mathrm{n}_{\mathrm{NaBH_4}} = \mathrm{c} \times \mathrm{V} = 0.1\ \frac{mol}{l}\ \times 0.1 \times 10^{-3} l = 0.1\ \times 10^{-4}\ (mol)$$

Since $NaBH_4$ was used up, the mole of Fe^0 would be calculated according to the mole of $NaBH_4$ (equation 5):

$$\mathrm{n}_{\mathrm{Fe^0}} = \frac{2\ mol_{\mathrm{Fe^0}}}{6\ mol_{\mathrm{NaBH_4}}} \times \mathrm{n}_{\mathrm{NaBH_4}} = \frac{2\ mol_{\mathrm{Fe^0}}}{6\ mol_{\mathrm{NaBH_4}}} \times 0.1\ \times 10^{-4}\ mol = 3.33 \times 10^{-6}\ (mol)$$

The mass of nZVI formed in 1h was:

$$\mathrm{m}_{\mathrm{Fe^0}} = \mathrm{n} \times \mathrm{M} = 3.33 \times 10^{-6}\ mol \times 56 \frac{g}{mol} = 1.86 \times 10^{-4}\ (g)$$

Therefore, the mass of nZVI formed in 1 minute was:

$$\mathrm{m}_{\mathrm{Fe^0}}\ \text{per minute} = \frac{\mathrm{m}_{\mathrm{Fe^0}}\ \text{in 1h}}{60\ \text{minutes}} = \frac{1.86 \times 10^{-4}\ g/h}{60\ min} = 3.11 \times 10^{-6}\ (\frac{g}{min})$$

Appendix 2. UV-vis data for MO

TABLE 5. Absorbance of MO after treatment in different times at wavelength of 464 nm

Synthesis time (min)	Absorbance (Au)
0	1,67088
10	1,16427
20	0,39098
30	0,32916
40	0,02205

TABLE 6. Absorbance of MO after treatment with different pH at wavelength of 464 nm

pH	Absorbance (Au)
1	0,50126
3	0,08354
5	0,55874
7	0,6336
9	0,88156
11	1,00386

Appendix 3. UV-vis data for MB

TABLE 7. Absorbance of MB after treatment in different times at wavelength of 665 nm

Synthesis time (min)	Absorbance (Au)
0	0,16718
2	0,08278
4	0,04946
6	0,03213
8	0,02065
10	0,01017

TABLE 8. Absorbance of MB after treatment with different pH at wavelength of 665 nm

pH	Absorbance (Au)
1	0,03123
3	0,09813
5	0,09011
7	0,03509
9	0,02727
11	0,02774